Synthesis, Characterization, and Molecular Docking Study of Some Novel Imidazole Derivatives as Potential Antifungal Agents

Ayşen Işık,[a] Ulviye Acar Çevik,[a,b] Begüm Nurpelin Sağlık,[a,b] and Yusuf Özkay[a,b]*

[a]Department of Pharmaceutical Chemistry, Faculty of Pharmacy, Anadolu University, 26470 Eskişehir, Turkey
[b]Doping and Narcotic Compounds Analysis Laboratory, Faculty of Pharmacy, Anadolu University, 26470 Eskişehir, Turkey
*E-mail: yozkay@anadolu.edu.tr

Received May 23, 2018
DOI 10.1002/jhet.3388
Published online 00 Month 2018 in Wiley Online Library (wileyonlinelibrary.com).

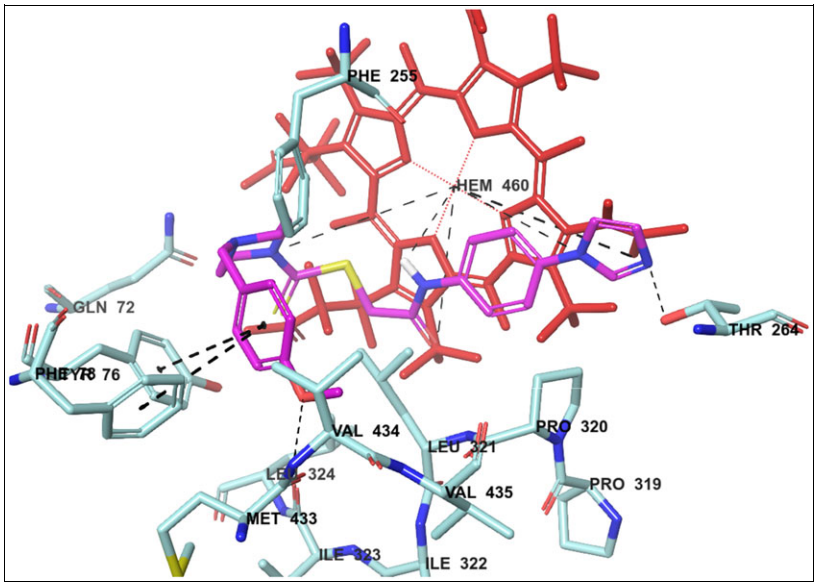

The azole pharmacophore is still regarded as a viable lead structure for the synthesis of more effective antifungal agents. In this study, two novel series of imidazole derivatives containing dithiocarbamate **(5a–5g)** and (benz)azolethiol **(6a–6n)** side chains that are structurally related to the famous antifungal azole pharmacophore were synthesized, and the structures of them were characterized by spectral (IR, ^{1}H NMR, ^{13}C NMR, and MS spectra) analyses. The synthesized compounds were screened *in vitro* antifungal activity against pathogenic strains fungi. Theoretical ADME (absorption, distribution, metabolism, and excretion) predictions were calculated for final compounds. A molecular docking study of the most active compound with target "lanosterol 14α-demethylase" (CYP51) was performed to unravel the mode of antifungal action. Compound **5e**, which features imidazole and 4-methoxybenzyl piperazine scaffolds, showed the most promising antifungal activity with an MIC_{50} value of 0.78 μg/mL against *C. krusei*. Effect of the compound **5e** against ergosterol biosynthesis was observed by LC–MS–MS method, which is based on quantification of ergosterol level in *C. krusei*.

INTRODUCTION

In recent years, the incidences of systemic fungal infections are increasing dramatically as a consequence of various factors, including the indiscriminate use of antibiotics, the extensive practice of organ transplants, and the rise in drug addiction and disease that suppress the immune system [1–3]. Currently, the available antifungal agents to treat fungal infections can be divided into four categories based on their mode of action, including the polyenes (e.g., amphotericin B and nystatin) [4], echinocandins (e.g., caspofungin and micafungin) [5], azoles (e.g., ketoconazole, fluconazole, voriconazole, and itraconazole) [6], and antimetabolites (e.g., 5-fluorocytosine) [7]. Among these agents, azole groups are most widely used in antifungal therapy [8].

Azole antifungal drugs mainly act by inhibiting CYP51 or lanosterol-14α-demethylase, an enzyme necessary in ergosterol biosynthesis, through a mechanism in which the heterocyclic nitrogen of the azole binds (N-3 of imidazole) as the sixth ligand to the heme iron present in the enzyme, thereby altering the structure of the active site and acting as non-competitive inhibitors. In addition to the N-3 of imidazole, a second nitrogen is thought to interact directly with the apoprotein of lanosterol demethylase. It is thought that the position of this second nitrogen in relation to the apoprotein may determine the specificity of different azole drugs for the enzyme [9–11].

© 2018 Wiley Periodicals, Inc.

The accumulation of 14-α-methylated sterols and depletion of ergosterol alter membrane fluidity, thereby increasing its permeability. The effectiveness of azoles as inhibitors of the 14-α-demethylase has been supported through several experiments [12–16].

In addition to the azole group, dithiocarbamates are a well-known class of compounds that have been shown to possess antifungal activity [17]. It has been reported that thiocarbamate derivatives disturbed the cell wall biosynthesis of the pathogen by inhibiting the ergosterol biosynthesis [18]. In recent studies, the compounds in which dithiocarbamate moiety was combined with different heterocycles became promising candidates for new antifungal agent investigation [19–24].

Clinically, representative antifungal drugs have certain limitation such as narrow spectrum of activity, non-optimal pharmacokinetics, and the emergence of drug resistance (generally azoles). Therefore, there is an urgent need for development of antifungal agents of new molecular scaffolds with high efficiency, broad spectrum, and optimal pharmacokinetics that are highly desirable [25,26].

In the current work, in order to take the advantage of the antifungal properties of imidazoles, we synthesized new 2-substituted-*N*-[4-(1*H*-imidazole-1-yl)phenyl]acetamide (**5a–5g**, **6a–6n**) derivatives and evaluated antifungal activities of these compounds.

RESULTS AND DISCUSSION

Chemistry. In the synthetic procedure of the 2-substituted-*N*-[4-(1*H*-imidazole-1-yl)phenyl]acetamide (**5a–g**, **6a–n**) derivatives, initially microwave supported synthesis of 1-(4-nitrophenyl)-1*H*-imidazole (**1**) was performed in DMF. In the next step, reduction of compound **1** by Zn/HCl in EtOH gave 1-(4-aminophenyl)-1*H*-imidazole (**2**), which was then acetylated with chloroacetyl chloride in conventional ways to afford 2-chloro-*N*-[4-(1*H*-imidazole-1-yl)phenyl]acetamide (**3**). Compound **3** was reacted with dithiocarbamate sodium salts (**4a–4g**) or (benz)azolethiol derivatives in acetone to obtain target compounds (**5a–5g**, **6a–6n**). Synthetic route for the final compounds was outlined in Scheme 1. Structure elucidations of the final compounds (**5a–g**, **6a–n**) were performed by FT-IR, ^{1}H-NMR, ^{13}C-NMR, and MASS spectroscopic methods. The stretching bands for C=O and C=S were observed between 1622 and 1691 cm^{-1} and 1200 and 1246 cm^{-1}, respectively. Stretching absorption of N–H groups was observed at 3041–3305 cm^{-1} as expected. The stretching absorption at about 1419–1639 cm^{-1} was recorded for C=C and C=N double bonds in heteroaromatic rings. The stretching absorption belonging to 1,4-disubstituted benzene was determined at 813–843 cm^{-1}.

In the ^{1}H-NMR spectra, piperazine was seen between 3.38 and 4.32 ppm as three singlet peaks. Conformational mobility of cyclic compounds is greatly limited; therefore, less rotational averaging of various chemical shift anisotropic effects occurs. Thus, the chemical shift values of the equatorial and axial hydrogens of the piperazine ring were seen at different regions as different 2H, 2H, and 4H peaks in agreement with the literature [27]. Methylene protons between carbonyl and dithioate groups were recorded as a singlet peak between 4.26 and 4.32 ppm. N–H proton of amide group gave singlet at 10.45–10.50 ppm, and aromatic protons were observed in the range of 6.89–8.40 ppm. The protons of the methyl ($-CH_3$) and methoxy ($-OCH_3$) substituents were observed as a singlet peak between 2.34 and 2.49 ppm and 3.82 and 3.89 ppm, respectively. In the ^{13}C-NMR spectra, peaks about 195 and 165 ppm were assigned to carbon atoms of C=S and C=O groups, respectively. In the HRMS spectra, all measured mass and isotope scores were compatible with calculated values for the compounds (**5a–g**).

Antifungal activity. The target compounds were evaluated for their antifungal activity against *C. albicans* (ATCC 24433), *C. krusei* (ATCC 6258), *C. parapsilosis* (ATCC 22019), and *C. glabrata* (ATCC 90030) according to the protocol of the EUCAST [28]. Broth microdiluation methods were used to determine the minimum inhibitory concentrations (MICs) of the final compounds in 96-well microtest plates. MIC_{50} values were evaluated *via* fluorometric measurements, using resazurin solution [29,30]. Ketoconazole and fluconazole were used as reference drugs. The *in vitro* antifungal activities of the synthesized compounds were listed in Table 1.

In terms of chemical structure, synthesized compounds can be separated in two main groups. The first group includes the compounds **5a–5g**, which carry dithiocarbamate side chain. In the second group, the compounds **6a–6n** bear (benz) azolethiol substructure. In general, the compounds in the first group displayed better antifungal activity than the compounds in the second group. The compounds **5a–5g** indicated comparable anticandidal activity to reference drugs ketoconazole and fluconazole. *C. krusei* (ATCC 6258) was the most sensitive fungal strain against these compounds. Compound **5e** showed the most potent activity against *C. krusei* (ATCC 6258), with an MIC_{50} value of 0.78 μg/mL, while the MIC_{50} value of the reference drugs was 1.56 μg/mL against same *Candida* strain.

In terms of short structure activity relationships, it is observed that 4-benzylpiperazine moiety in the dithiocarbamate side chain of compounds **5d** and **5e** makes higher contribution to anticandidal effect when compared with other moieties. Furthermore, 4-methoxy substitution of benzyl fragment in compound **5e** enhances the anticandidal activity.

Scheme 1. Synthesis way for target compounds.

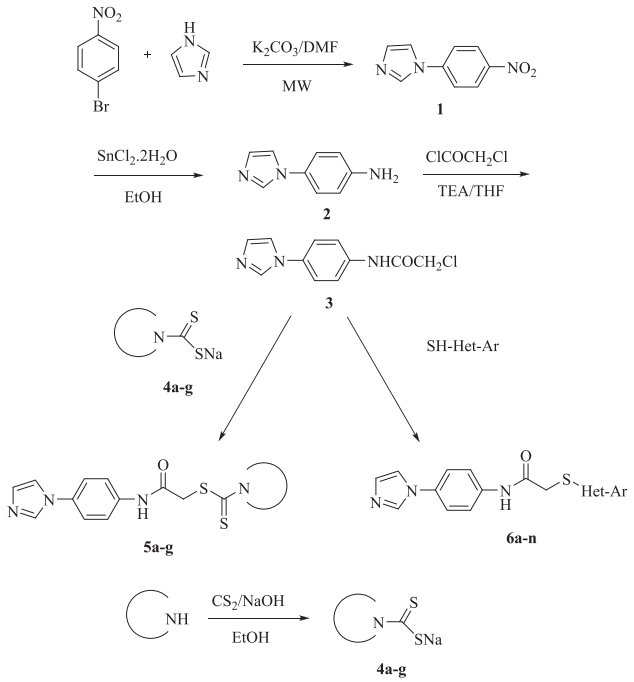

Comp.		Comp.	
5a	Piperidine	**6e**	5-Chlorobenzimidazole
5b	4-Benzylpiperidine	**6f**	Benzothiazole
5c	4-Methylpiperidine	**6g**	5-Methoxybenzothiazole
5d	4-Benzylpiperazine	**6h**	5-Chlorobenzothiazole
5e	4-Methoxy-benzylpiperazine	**6ı**	1-Methylimidazole
5f	4-Nitro-phenylpiperazine	**6j**	2-Methyl-1,3,4-thiadiazole
5g	4-Fluoro-phenylpiperazine	**6k**	1,2,4-triazole
6a	Benzimidazole	**6l**	4-Methyl-1,2,4-triazole
6b	5-Methylbenzimidazole	**6m**	1-Methyltetrazole
6c	5-Nitrobenzimidazole	**6n**	2-Methylpyrimidine
6d	5-Methoxybenzimidazole		

Inhibition of ergosterol biosynthesis. Infections caused by eukaryotic organisms like fungus generally present more difficult treatment problems than those of bacterial infections. There are relatively few antifungal drugs that can identify unique targets not shared with human hosts. The fungal cell wall remains an underdeveloped therapeutic target for selective antifungal agents because of its chitin structure, which is absent in human cells [16,31].

The present work is an attempt to understand the mechanism of antifungal activity of newly synthesized imidazole-dithiocarbamate hybrid compound **5e**. Most therapies, designed to treat fungal infections, target the ergosterol biosynthesis pathway. It is the main sterol of fungi cell membranes and is necessary for fluidity, permeability, and protein function [32], and hence, inhibition of ergosterol biosynthesis causes the end of life functions.

For quantitative determination of ergosterol level of *C. krusei*, we used an LCMSMS method. Total intracellular sterols were extracted as reported by Breivik and Owades [33]. Ergosterol standard (product no. 45480, Sigma-Aldrich, Germany) was used for quantification of ergostrerol in both inhibitor-free (negative control) and inhibitor including samples. The most active compound **5e** and reference drugs were used at 0.78-, 1.56-, and 3.12-μg/mL concentrations. Ergosterol quantity in negative control samples was regarded as 100%. All concentrations were analyzed in quadruplicate, and the results were expressed as mean ± standard deviation (Fig. 1).

Ergosterol quantification studies revealed that compound **5e** and reference agents significantly decreased the level of ergosterol at all tested concentrations. A concentration-dependant decrease in the ergosterol level was established for all tested agents. Hence, it can be obviously suggested that compounds **5e** have a role in the ergosterol biosynthesis pathway.

Prediction of ADME parameters. Most of new drug candidates fail in clinical trials because of their poor ADME (absorption, distribution, metabolism, and excretion) properties. These late-stage failures contribute significantly to the rapidly increasing cost of new drug

Table 1

MIC_{50} (μg/mL) values of compounds (**5a–g**, **6a–n**).

Comp.	*C. albicans*	*C. glabrata*	*C. krusei*	*C. parapsilosis*
5a	6.25	3.125	1.56	6.25
5b	25	6.25	3.125	6.25
5c	3.125	6.25	3.125	6.25
5d	3.125	3.125	1.56	3.125
5e	1.56	3.125	0.78	1.56
5f	12.5	12.5	3.125	6.25
5g	12.5	6.25	3.125	12.5
6a	200	200	200	200
6b	200	200	200	200
6c	25	200	200	100
6d	100	200	200	200
6e	200	200	200	200
6f	200	200	200	100
6g	100	200	200	100
6h	200	200	200	100
6i	200	200	200	200
6j	200	200	200	100
6k	100	200	200	200
6l	100	200	200	100
6m	100	200	200	200
6n	100	200	200	100
Ketoconazole	0.78	1.56	1.56	1.56
Fluconazole	0.78	1.56	1.56	0.78

development. The ability to detect problematic candidates early can dramatically reduce the amount of wasted time and resources and streamline the overall development process. Hence, pharmacokinetic profiles of the new drug candidates are very important and should be evaluated as early as possible in the drug development process. ADME prediction can be used to focus lead optimization efforts to enhance the desired properties of a given compound [34]. Thus, predictions of ADME properties of the all synthesized compounds (**5a–g**, **6a–n)** were performed by *QikProp 4.8* software [35].

This program applies the Lipinski's rule of five [36] and Jorgensen's rule of three [37], which evaluate the ADME properties of drug like compounds, and is important for the optimization of a biologically active compound. The theoretical calculations of ADME parameters (molecular weight, log P, polar surface area, number of hydrogen donors, number of hydrogen acceptors, number of rotatable bonds, and volume) are presented in Table 2 along with the violations of rules of three and five.

According to Lipinski's rule of five, all compounds (**5a–g**, **6a–n**) abide to the rule by causing no more than one violation. Also, these compounds are suited to Jorgensen's rule of three with no more than one violation. Besides, it can be seen that all results of rules of three and five are within recommended ranges. Thus, it can be suggested that all synthesized compounds may possess a good pharmacokinetic profile, increasing their pharmacological importance.

Molecular docking. Docking studies were performed in order to gain more insight into the binding modes of compound **5e** to 14-α-sterol demethylase, which is a key enzyme in ergosterol biosynthesis of fungi. Studies were carried out by using the X-ray crystal structure of 14-α-sterol demethylase from *Mycobacterium tuberculosis* in complex with fluconazole (PDB ID: 1EA1) [38].

According to the antifungal activity results, the compound **5e** shows significant antifungal activity against *C. krusei* with an MIC_{50} value of 0.78 μg/mL. Thus, the main purpose is to investigate the possible interaction of this compound with cytochrome P450 14-α-sterol demethylase from *C. krusei*. However, this enzyme is a membrane-bound enzyme, and it is difficult to crystalize for X-ray analysis and modeling studies. Moreover, there are no experimental data or crystal structure of this enzyme in Protein Data Bank server. On the other hand, in the database, there are two-analogous enzymes, origin

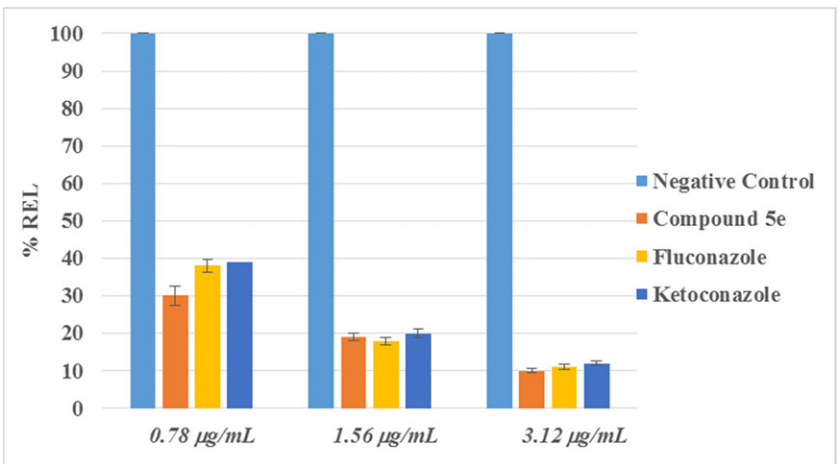

Figure 1. Relative ergosterol level (REL) of *Candida krusei* (ATCC 6258), after treatment with compound **5e**, fluconazole, and ketoconazole. [Color figure can be viewed at wileyonlinelibrary.com]

Table 2

Calculated ADME parameters (**5a–g**, **6a–n**).

Comp.	MW	RB	V	DHB	AHB	QPlogPo/w	PSA	VRF	VRT
5a	360.491	4	1.144.028	1	6	4.026	62.451	0	1
5b	450.616	6	1.404.067	1	6	5.885	61.658	1	1
5c	375.506	4	1.183.501	1	8	2.860	68.023	0	0
5d	451.603	6	1.414.058	1	8	4.512	67.883	0	1
5e	481.630	7	1.473.919	1	9	4.465	76.171	0	1
5f	482.574	5	1.437.640	1	8	4.471	117.017	0	1
5 g	455.567	4	1.371.342	1	7	5.414	68.352	1	1
6a	349.409	4	1.108.186	2	6	3.609	80.595	0	0
6b	363.436	4	1.166.642	2	6	3.903	80.419	0	1
6c	394.407	5	1.190.101	2	7	2.925	129.062	0	1
6d	379.436	5	1.176.943	2	6	3.675	89.076	0	1
6e	383.854	4	1.152.129	2	6	4.094	80.587	0	1
6f	366.455	4	1.130.869	1	6	4.219	65.645	0	1
6g	396.481	5	1.199.740	1	6	4.273	74.129	0	1
6h	400.900	4	1.174.760	1	6	4.709	65.643	0	1
6i	313.376	4	1.017.541	1	6	3.169	68.927	0	0
6j	331.410	4	1.035.668	1	6	2.956	81.796	0	0
6k	300.337	4	947.218	2	7	1.559	97.922	0	0
6l	314.364	4	1.004.941	1	7	1.703	85.311	0	0
6m	315.352	4	994.109	1	7	1.174	105.034	0	0
6n	311.361	4	1.001.472	1	6	2.857	76.386	0	0

MW, molecular weight; RB, number of rotatable bonds (recommended value: 0–15); V, total solvent-accessible volume in cubic angstroms using a probe with a 1.4-Å radius (recommended value: 500–2000); DHB, estimated number of hydrogen bonds that would be donated by the solute to water molecules in an aqueous solution (recommended value: 0–6); AHB, estimated number of hydrogen bonds that would be accepted by the solute from water molecules in an aqueous solution (recommended value: 2–20); QPlogPo/w, predicted octanol/water partition coefficient (recommended value: −2–6.5); PSA, Van der Waals surface area of polar nitrogen and oxygen atoms and carbonyl carbon atoms (recommended value: 7–200); VRF, number of violations of Lipinski's rule of five [36]. The rules are mol_MW $<$ 500, QPlogPo/w $<$ 5, donorHB $\leq$ 5, and accptHB $\leq$ 10. Compounds that satisfy these rules are considered druglike. (The "five" refers to the limits, which are multiples of 5.) (Maximum is 4); VRT, number of violations of Jorgensen's rule of three [37]. The three rules are QPlogS $>$ −5.7, QP PCaco $>$ 22 nm/s, and # primary metabolites $<$ 7. Compounds with fewer (and preferably no) violations of these rules are more likely to be orally available (maximum is 3).

of *Candida P450* and *Mycobacterium P450*. These enzymes have high homology and high degree of similarity between the hydrophobic cavities of the catalytic site [39–42]. Among them, *Mycobacterium P450* have been presented with higher resolution. Depending on these reasons, we choose the PDB ID: 1EA1 crystal structure from *M. tuberculosis* to obtain clearer pose (Fig. 2).

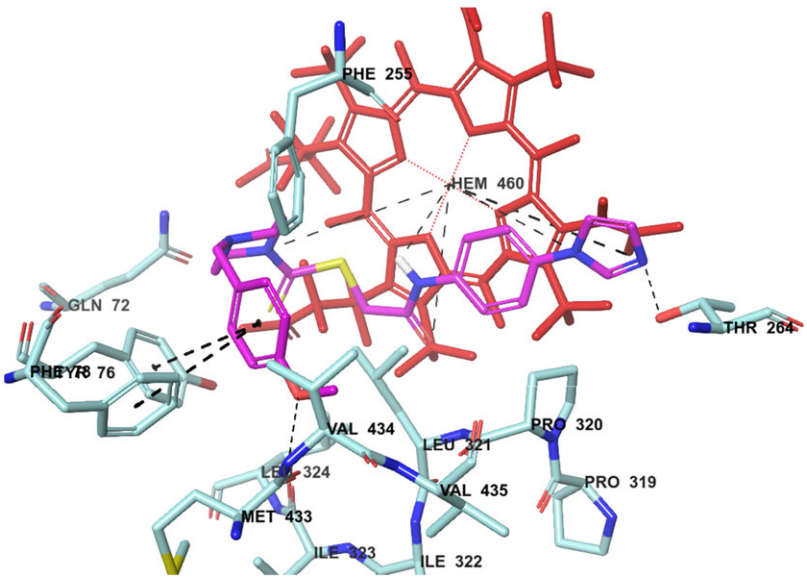

Figure 2. The interacting mode of compound **5e** in the active region of 14 alpha-sterol demethylase. The inhibitor is colored with purple and HEM with red. [Color figure can be viewed at wileyonlinelibrary.com]

The docking pose on 14-α-sterol demethylase reveals that the interactions between the compound **5e** and HEM450 are very important in terms of binding to active site of enzyme (Fig. 2). The HEM450 establishes five metal coordination bonds with the 1st nitrogen of piperazine, the carbonyl and amino groups of amide function, and two nitrogens of imidazole ring. The 3rd nitrogen of imidazole has a part in polar interactions along with metal bond. There is a hydrogen bond between this nitrogen and Thr264. Also, phenyl ring creates two π–π interaction with the phenyl of Tyr76 and Phe78. The methoxy group creates a hydrogen bond with the amino group of Val434. This interaction emphasizes why the compound **5e** is more active than the other synthesized derivatives. The methoxy group helps to strengthen the polar interaction differently from other substituents.

CONCLUSIONS

In summary, we discovered a novel class of compounds indicating important anticandidal effects. In addition to good antifungal activity, all compounds in the series exhibited a good predicted pharmacokinetics profile. Furthermore, preliminary mechanism of action study showed that the potent antifungal activity of compound **5e** is related to inhibition of ergosterol biosynthesis in *C. krusei*. Significant interactions were also observed between compound **5e** and 14-α-sterol demethylase. We expect that in further studies, all these findings may have an effect on medicinal chemists to discover more promising anticandidal compounds.

EXPERIMENTAL

Chemistry. All of the chemicals used in the study were purchased from either Sigma-Aldrich Corp. (St. Louis, MO) or Merck KGaA (Darmstadt, Germany) and used without further chemical purifications. Microwave syntheses were realized by using a Monowave 300 high-performance microwave reactor (Anton-Paar, Austria). Melting points of the synthesized compounds were determined by using a MP90 series automatic melting point determination system (Mettler-Toledo, OH) and were presented as uncorrected. ^{1}H and ^{13}C NMR spectra were recorded in DMSO-d_6 by a Bruker digital FT-NMR spectrometer (Bruker Bioscience, Billerica, MA) at 300, 75 or 500, and 125 MHz [splitting patterns in the NMR spectra were designated as follows: s, singlet; d, doublet; t, triplet; m, multiplet; coupling constants (*J*) were reported in Hertz]. The IR spectra of the compounds were recorded using an IRAffinity-1S Fourier transform IR (FTIR) spectrometer. HRMS studies were performed on Shimadzu LCMS-IT-TOF system (Shimadzu, Tokyo, Japan). LC–MS–MS studies were performed on a Schimadzu, 8040 LC–MS–MS spectrophotometer (Shimadzu, Tokyo, Japan). Chemical purities of the compounds were checked by classical TLC applications performed on silica gel 60 F_{254} (Merck KGaA).

General procedure for 1-(4-nitrophenyl)-1*H*-*imidazole (1)*. 1-Iodo-4-nitrobenzene (9.96 g, 0.04 mol), K_2CO_3 (5.52 g, 0.04 mol), 1*H*-imidazole (2.72 g, 0.04 mol) in DMF (10 mL) were put into a vial (30 mL) of microwave synthesis reactor (Anton-Paar Monowave 300). The reaction mixture was kept under the conditions of 200°C and 10 bar for 15 min. After cooling, the mixture was poured into iced-water; precipitated product was washed with water, dried, and recrystallized from ethanol. Yield: 89%; m.p. 201–204°C. Literature m.p. 203°C [43].

General procedure for 1-(4-aminophenyl)-1*H*-*imidazole (2)*. 1-(4-Nitrophenyl)-1*H*-imidazole (**1**) (6.62 g, 0.035 mol) was dissolved in ethanol (50 mL), and 25% HCl (50 mL) was added. Zinc powder (39.49 g, 0.35 mol) was divided into 10 equal portions, and each portion was added to the stirring solution in 15-min intervals. Once the addition of the zinc was completed, reaction mixture was refluxed for 1 h. After cooling, the mixture was poured into iced-water and then neutralized by using 10% NaOH solution. The precipitate was extracted with ethyl acetate in portions (3 × 100 mL). Extracts were combined and dried with anhydrous sodium sulfate. The solvent was evaporated, and the residue was recrystallized from ethanol to give the 1-(4-aminophenyl)-1*H*-imidazole (**2**). Yield: 71%; m.p. 142–144°C. Literature m.p. 141–143°C [44].

General procedure for *N-[4-(1*H*-imidazol-1-yl)phenyl]-2-chloro-acetamide (3)*. 1-(4-Aminophenyl)-1*H*-imidazole (**2**) (3.18 g, 0.02 mol) and triethylamine (3.1 mL, 0.022 mol) in THF (100 mL) were allowed to stir on an ice bath. Chloroacetylchloride (1.75 mL, 0.022 mol) in THF (10 mL) was added drop by drop. After this stage, the content was stirred for 1 h at room temperature. THF was evaporated, and the product was recrystallized from ethanol. Yield: 75%; m.p. 230–234°C.

General procedure for the synthesis of sodium dithiocarbamate derivatives (4a–g). Secondary amine derivative (0.01 mol) and sodium hydroxide (0.4 g, 0.01 mol) in ethanol (10 mL) were cooled in an ice bath, and CS_2 (6 mL) was added drop by drop. The reaction was allowed to stir for 1 h at room temperature. The solvent and excess of CS_2 were removed under reduced pressure. The residue was washed with dry ether, and the raw product was recrystallized from ethanol.

General procedure for the synthesis of 2-(substitute ddithiocarbamoyl)-*N*-[4-(1*H*-imidazol-1-yl)phenyl]acetamide derivatives (5a–g). Corresponding sodiumdithiocarbamate

(**4a–g**) (0.001 mol) and *N*-[4-(1*H*-imidazol-1-yl)phenyl]-2-chloro-acetamide (**3**) (0.24 g, 0.001 mol) in acetone were refluxed for 2 h. After TLC control, the solvent was evaporated; the residue was washed with water, dried, and then recrystallized from ethanol to afford final compounds (**5a–g**).

2-(Piperidine-1-yl-dithiocarbamoyl)-N-[4-(1H-imidazol-1-yl) phenyl]acetamide (5a). Yield: 83%; m.p. 165.6–170.2°C. FTIR (ATR, cm^{-1}): 3041 (N–H), 1691 (C=O), 1228 (C=S), 842 (1,4-disubstituted benzene). ^{1}H-NMR (300 MHz) (DMSO-d_6) δ (ppm): 10.45 (1H, s, N–H), 8.18 (1H, s, imidazole, C_2-H), 7.70 (2H, d, J = 8.7 Hz, 1,4-disubstituted benzene), 7.68 (1H, s, imidazole-C_5-H), 7.58 (2H, d, J = 8.7 Hz, 1,4-disubstituted benzene), 7.09 (1H, s, imidazole-C_4-H), 4.26 (2H, s, –CH_2–), 4.20 (2H, s, piperidine –CH_2–), 3.94 (2H, s, piperidine –CH_2–), 1.60 (6H, br.s, piperidine –CH_2–). ^{13}C-NMR (75 MHz, DMSO-d_6): δ (ppm): 23.94, 25.66, 26.29, 41.75, 51.53, 53.04, 118.48, 120.50, 121.31, 130.14, 132.69, 135.83, 138.22, 166.06, 193.46. $[M + H]^+$ calcd for $C_{17}H_{20}N_4OS_2$: 361.1151; found: 361.1146.

2-(4-Benzylpiperidine-1-yl-dithiocarbamoyl)-N-[4-(1H-imidazol-1-yl)phenyl]acetamide (5b). Yield: 78%; m.p. 86.8–90.8°C. FTIR (ATR, cm^{-1}): 3109 (N–H), 1681 (C=O), 1232 (C=S), 815 (1,4-disubstituted benzene). ^{1}H-NMR (300 MHz) (DMSO-d_6) δ (ppm): 10.48 (1H, s, N–H), 8.19 (1H, s, imidazole, C_2-H), 7.71 (2H, d, J = 8.7 Hz, 1,4-disubstituted benzene), 7.68 (1H, s, imidazole-C_5-H), 7.58 (2H, d, J = 8.7 Hz, 1,4-disubstituted benzene), 7.27 (2H, d, J = 6.9 Hz, phenyl H_2, H_6), 7.19–7.17 (3H, m, phenyl H_3, H_4, H_5), 7.09 (1H, s, imidazole-C_4-H), 4.26 (2H, s, –CH_2–), 2.55–2.50 (4H, m, piperidine –CH_2–, –CH_2), 1.92 (1H, br.s, piperidine –CH–), 1.70 (3H, br.s, piperidine –CH_2–), 1.24–1.17 (3H, m, piperidine, –CH_2). ^{13}C-NMR (75 MHz, DMSO-d_6): δ (ppm): 35.36, 37.35, 41.83, 41.95, 43.55, 50.56, 52.12, 118.49, 120.49, 121.31, 126.39, 128.68, 129.49, 130.11, 132.68, 135.83, 138.24, 140.33, 166.04, 193.60. $[M + H]^+$ calcd for $C_{24}H_{26}N_4OS_2$: 451.1621; found: 451.1621.

2-(4-Methylpiperazine-1-yl-dithiocarbamoyl)-N-[4-(1H-imidazol-1-yl)phenyl]acetamide (5c). Yield: 86%; m.p. 131.3–134.9°C. FTIR (ATR, cm^{-1}): 3118 (N–H), 1689 (C=O), 1238 (C=S), 815 (1,4-disubstituted benzene). ^{1}H-NMR (300 MHz) (DMSO-d_6) δ (ppm): 10.76 (1H, s, N–H), 8.24 (1H, s, imidazole, C_2-H), 7.75 (1H, s, imidazole-C_5-H), 7.72 (2H, d, J = 8.7 Hz, 1,4-disubstituted benzene), 7.60 (2H, d, J = 8.7 Hz, 1,4-disubstituted benzene), 7.11 (1H, s, imidazole-C_4-H), 4.26 (2H, s, –CH_2–), 4.31 (2H, br.s, piperazine –CH_2–), 4.15 (2H, br.s, piperazine –CH_2–), 3.40 (4H, br.s, piperazine –CH_2–), 2.49 (3H, s, CH_3). ^{13}C-NMR (75 MHz, DMSO-d_6): δ (ppm): 13.94, 41.88, 43.85, 48.68, 53.14, 118.60, 120.54, 121.41, 129.85, 132.72, 135.83, 138.20, 165.52, 193.52. $[M + H]^+$ calcd for $C_{17}H_{21}N_5OS_2$: 376.1260; found: 376.1252.

2-(4-Benzylpiperazine-1-yl-dithiocarbamoyl)-N-[4-(1H-imidazol-1-yl)phenyl]acetamide (5d). Yield: 81%; m.p. 90.4–94.8°C. FTIR (ATR, cm^{-1}): 3116 (N–H), 1674 (C=O), 1228 (C=S), 833 (1,4-disubstituted benzene). ^{1}H-NMR (300 MHz) (DMSO-d_6) δ (ppm): 10.44 (1H, s, N–H), 8.18 (1H, s, imidazole, C_2-H), 7.70 (2H, d, J = 8.8 Hz, 1,4-disubstituted benzene), 7.68 (1H, s, imidazole-C_5-H), 7.58 (2H, d, J = 8.8 Hz, 1,4-disubstituted benzene), 7.26 (2H, d, J = 6.9 Hz, phenyl H_2, H_6), 7.18–7.12 (3H, m, phenyl H_3, H_4, H_5), 7.08 (1H, s, imidazole-C_4-H), 4.26 (2H, s, –CH_2–), 4.20 (2H, br.s, piperazine –CH_2–), 3.94 (2H, br.s, piperazine –CH_2–), 3.35 (4H, br.s, piperazine –CH_2–), 2.42 (2H, s, –CH_2). ^{13}C-NMR (75 MHz, DMSO-d_6): δ (ppm): 41.70, 50.28, 51.59, 52.39, 61.73, 118.49, 120.50, 121.28, 127.60, 128.72, 129.43, 130.12, 132.67, 135.84, 137.96, 138.26, 165.96, 194.80. $[M + H]^+$ calcd for $C_{23}H_{25}N_5OS_2$: 452.1573; found: 452.1565.

2-(4-(4-Methoxybenzyl)piperazine-1-yl-dithiocarbamoyl)-N-[4-(1H-imidazol-1-yl)phenyl]acetamide (5e). Yield: 75%; m. p. 184.5–187.9°C. FTIR (ATR, cm^{-1}): 3097 (N–H), 1683 (C=O), 1224 (C=S), 823 (1,4-disubstituted benzene). ^{1}H-NMR (300 MHz) (DMSO-d_6) δ (ppm): 10.47 (1H, s, N–H), 8.18 (1H, s, imidazole, C_2-H), 7.71 (2H, d, J = 8.8 Hz, 1,4-disubstituted benzene), 7.68 (1H, s, imidazole-C_5-H), 7.58 (2H, d, J = 8.8 Hz, 1,4-disubstituted benzene), 7.22 (2H, d, J = 8.4 Hz, 1,4-disubstituted benzene), 7.09 (1H, s, imidazole-C_4-H), 6.89 (2H, d, J = 8.4 Hz, 1,4-disubstituted benzene), 4.27 (2H, s, –CH_2–), 4.21 (2H, br.s, piperazine –CH_2–), 3.95 (2H, br.s, piperazine –CH_2–), 3.73 (3H, s, OCH_3–), 3.40 (4H, br.s, piperazine –CH_2), 2.45 (2H, s, –CH_2). ^{13}C-NMR (75 MHz, DMSO-d_6): δ (ppm): 41.71, 50.27, 51.59, 52.23, 55.48, 61.12, 114.08, 118.48, 120.50, 121.32, 129.65, 130.13, 130.72, 132.70, 135.83, 138.21, 158.88, 165.94, 194.73. $[M + H]^+$ calcd for $C_{24}H_{27}N_5O_2S_2$: 482.1679; found: 482.1677.

2-(4-(4-Nitrophenyl)piperazine-1-yl-dithiocarbamoyl)-N-[4-(1H-imidazol-1-yl)phenyl]acetamide (5f). Yield: 84%; m.p. 146.8–150.4°C. FTIR (ATR, cm^{-1}): 3109 (N–H), 1689 (C=O), 1219 (C=S), 821 (1,4-disubstituted benzene). ^{1}H-NMR (300 MHz) (DMSO-d_6) δ (ppm): 10.50 (1H, s, N–H), 8.19 (1H, s, imidazole, C_2-H), 8.10 (2H, d, J = 9.3 Hz, 1,4-disubstituted benzene), 7.71 (2H, d, J = 8.7 Hz, 1,4-disubstituted benzene), 7.68 (1H, s, imidazole-C_5-H), 7.59 (2H, d, J = 8.7 Hz, 1,4-disubstituted benzene), 7.09 (1H, s, imidazole-C_4-H), 6.95 (2H, d, J = 9.3 Hz, 1,4-disubstituted benzene), 4.32 (4H, s, –CH_2–, piperazine –CH_2–), 4.17 (2H, br.s, piperazine –CH_2–), 3.73 (4H, br.s, piperazine –CH_2–). ^{13}C-NMR (75 MHz, DMSO-d_6): δ (ppm): 41.60, 42.77, 44.11, 45.16, 112.31, 113.87, 118.49, 121.33, 126.27, 130.11, 132.71, 135.83, 137.30, 138.21, 154.16, 165.87, 195.18. $[M + H]^+$ calcd for $C_{22}H_{22}N_6O_3S_2$: 483.1268; found: 483.1265.

2-(4-(4-Fluorophenyl)piperazine-1-yl-dithiocarbamoyl)-N-[4-(1H-imidazol-1-yl)phenyl]acetamide (5g). Yield: 77%; m.p. 187.2–190.2°C. FTIR (ATR, cm^{-1}): 3049 (N–H), 1670 (C=O), 1217 (C=S), 813 (1,4-disubstituted benzene). ^{1}H-NMR (300 MHz) (DMSO-d_6) δ (ppm): 10.48 (1H, s, N–H), 8.18 (1H, s, imidazole, C_2-H), 7.71 (2H, d, J = 8.8 Hz, 1,4-disubstituted benzene), 7.68 (1H, s, imidazole-C_5-H), 7.59 (2H, d, J = 8.8 Hz, 1,4-disubstituted benzene), 7.08–7.05 (3H, m, 1,4-disubstituted benzene, imidazole-C_4-H), 7.00–6.99 (2H, m, 1,4-disubstituted benzene), 4.31 (4H, s, –CH_2–, piperazine –CH_2–), 4.13 (2H, br.s, piperazine –CH_2–), 3.38 (4H, br.s, piperazine –CH_2–). ^{13}C-NMR (75 MHz, DMSO-d_6): δ (ppm): 41.69, 48.96, 50.01, 51.19, 115.91 (d, J = 21.8 Hz), 117.93 (d, J = 7.5 Hz), 118.49, 120.51, 121.33, 130.13, 132.72, 135.84, 138.20, 147.21, 156.78 (d, J = 234.75 Hz), 165.91, 195.09. $[M + H]^+$ calcd for $C_{22}H_{22}N_5OFS_2$: 456.1323; found: 456.1325.

General procedure for the synthesis of 2-(mercaptoheteroaryl)-*N*-[4-(1*H*-imidazol-1-yl)phenyl]acetamide derivatives (6a–n). An appropriate (benz)azole-thiol (0.001 mol), *N*-[4-(1*H*-imidazol-1-yl)phenyl]-2-chloro-acetamide (**3**) (0.24 g, 0.001 mol), and K_2CO_3 (0.138 g, 0.001 mol) in acetone were refluxed for 2 h. After TLC control, the solvent was evaporated; the residue was washed with water, dried, and then recrystallized from ethanol to afford final compounds (**6a–n**).

2-(2-Mercaptobenzimidazole)-N-[4-(1H-imidazol-1-yl) phenyl]acetamide (6a). Yield: 76%; m.p. 230.8–232.7°C. FTIR (ATR, cm^{-1}): 3223 (N–H), 1641 (C=O), 1612–1440 (C=C and C=N), 835 (1,4-disubstituted benzene). ^{1}H-NMR (500 MHz) (DMSO-d_6) δ (ppm): 4.30 (2H, s, CH_2-S), 7.08 (1H, s, imidazole, C_5-H), 7.11–7.15 (2H, m, benzimidazole, $C_{5,6}$-H), 7.40–7.49 (2H, m, benzimidazole, $C_{4,7}$-H), 7.60 (2H, d, J = 9.0 Hz, phenyl, $C_{2,6}$-H), 7.68 (1H, s, imidazole, C_4-H), 7.71 (2H, d, J = 9.0 Hz, phenyl, $C_{3,5}$-H), 8.18 (1H, s, imidazole, C_2-H), 10.67 (1H, s, NH-CO), 12.67 (1H, s, benzimidazole-NH). ^{13}C-NMR (125 MHz, DMSO-d_6) δ (ppm): 36.1, 114.6, 118.0, 120.0, 120.9, 129.7, 132.4, 135.4, 137.6, 139.3, 149.0, 149.8, 166.3. LCMS (ESI) *m/z*: 175.60 (% 100.00), 350.15 (% 92.02), 351.15 (% 34.36), 352.10 (% 11.37).

2-(2-Mercapto-5-methylbenzimidazole)-N-[4-(1H-imidazol-1-yl)phenyl]acetamide (6b). Yield: 73%; m.p. 202.5–204.1°C. FTIR (ATR, cm^{-1}): 3122 (N–H), 1672 (C=O), 1618–1467 (C=C and C=N), 835 (1,4-disubstituted benzene). ^{1}H-NMR (500 MHz) (DMSO-d_6) δ (ppm): 2.33 (3H, s, CH_3), 4.27 (2H, s, CH_2-S), 6.92–6.96 (3H, m, imidazole, C_5-H, benzimidazole, $C_{4,6}$-H), 7.01 (1H, d, J = 8.0 Hz, benzimidazole, C_7-H), 7.62 (2H, d, J = 9.0 Hz, phenyl, $C_{2,6}$-H), 7.73 (2H, d, J = 9.0 Hz, phenyl, $C_{3,5}$-H), 7.78 (1H, s, imidazole, C_4-H), 8.43 (1H, s, imidazole, C_5-H), 10.72 (1H, s, NH-CO), 12.41 (1H, s, benzimidazole-NH). ^{13}C-NMR (125 MHz, DMSO-d_6) δ (ppm): 21.2, 36.2, 109.1, 109.6, 118.5, 120.0, 121.2, 122.8, 123.2, 128.2, 130.2, 131.6, 131.9, 132.5, 135.2, 138.0, 166.4. LCMS (ESI) *m/z*: 182.60 (% 100.00), 364.15 (% 78.23), 365.15 (% 17.22), 366.30 (% 5.06).

2-(2-Mercapto-5-nitrobenzimidazole)-N-[4-(1H-imidazol-1-yl)phenyl]acetamide (6c). Yield: 73%; m.p. 202.5–204.1°C. FTIR (ATR, cm^{-1}): 3211 (N–H), 1669 (C=O), 1616–1453 (C=C and C=N), 819 (1,4-disubstituted benzene). ^{1}H-NMR (500 MHz) (DMSO-d_6) δ (ppm): 4.39 (2H, s, CH_2-S), 7.09 (1H, s, imidazole, C_5-H), 7.59–7.62 (3H, m, benzimidazole, C_7-H, phenyl $C_{2,6}$-H), 7.68 (1H,s, imidazole C_4-H), 7.73 (2H, d, J = 9.0 Hz, phenyl, $C_{3,5}$-H), 8.07 (1H, dd, J = 8.5 Hz, J = 2.5 Hz, benzimidazole, C_6-H), 8.18 (1H, s, imidazole, C_2-H), 8.31 (1H, d, J = 2.5 Hz, benzimidazole C_4-H), 10.63 (1H, s, NH-CO), 13.39 (1H, s, benzimidazole N–H). ^{13}C-NMR (125 MHz, DMSO-d_6) δ (ppm): 36.2, 110.5, 115.4, 117.5, 118.0, 120.1, 120.9, 129.7, 132.4, 135.4, 137.5, 138.4, 142.2, 145.8, 148.7, 165.8. LCMS (ESI) *m/z*: 198.05 (% 100.00), 350.15 (% 92.02), 351.15 (% 34.36), 352.10 (% 11.37).

2-(2-Mercapto-5-methoxybenzimidazole)-N-[4-(1H-imidazol-1-yl)phenyl]acetamide (6d). Yield: 79%; m.p. 228.4–230.8°C. FTIR (ATR, cm^{-1}): 3120 (N–H), 1674 (C=O), 1620–1413 (C=C and C=N), 827 (1,4-disubstituted benzene). ^{1}H-NMR (500 MHz) (DMSO-d_6) δ (ppm): 3.76 (3H, s, CH_3), 4.24 (2H, s, CH_2-S), 6.76 (1H, dd, J = 8.5 Hz, J = 2.5 Hz, benzimidazole, C_6-H), 6.92 (1H, br.s, benzimidazole, C_4-H), 7.08 (1H, t, J = 1.0 Hz, imidazole, C_5-H), 7.35 (1H, br.s, benzimidazole, C_7-H), 7.60 (2H, d, J = 9.0 Hz, phenyl, $C_{2,6}$-H), 7.67 (1H, t, J = 1.0 Hz, imidazole C_4-H), 7.71 (2H, d, J = 9.0 Hz, phenyl, $C_{3,5}$-H), 8.18 (1H, t, J = 1.0 Hz, imidazole C_2-H), 10.65 (1H, s, NH-CO), 12.51 (1H, s, benzimidazole-NH). ^{13}C-NMR (125 MHz, DMSO-d_6) δ (ppm): 36.3, 55.5, 102.5, 118.0, 120.0, 120.9, 122.3, 123.1, 129.7, 130.4, 131.2, 132.4, 135.4, 137.6, 145.8, 155.7, 166.3. LCMS (ESI) *m/z*: 190.60 (% 100.00), 380.10 (% 98.75), 381.15 (% 47.57), 382.10 (% 13.70).

2-(2-Mercapto-5-chlorobenzimidazole)-N-[4-(1H-imidazol-1-yl)phenyl]acetamide (6e). Yield: 62%; m.p. 232.5–234.2°C. FTIR (ATR, cm^{-1}): 2985 (N–H), 1672 (C=O), 1627–1523 (C=C and C=N), 839 (1,4-disubstituted benzene). ^{1}H-NMR (500 MHz) (DMSO-d_6) δ (ppm): 4.31 (2H, s, CH_2-S), 7.08–7.14 (3H, m, benzimidazole C-H), 7.16 (1H, s, imidazole, C_5-H), 7.60 (1H, d, J = 8.5 Hz, phenyl, $C_{2,6}$-H), 7.68 (1H, s, imidazole, C_4-H), 7.60 (2H, s, phenyl $C_{3,5}$-H), 8.18 (1H, s, imidazole, C_2-H), 10.62 (1H, s, NH-CO), 12.67 (1H, s, benzimidazole-NH). ^{13}C-NMR (125 MHz, DMSO-d_6) δ (ppm): 36.2, 108.1, 109.1, 110.5, 118.1, 120.0, 120.9, 122.2, 123.6, 126.6, 128.3, 128.8, 130.9, 131.3, 133.2, 166.5. LCMS (ESI) *m/z*: 192.55 (% 100.00), 193.40 (% 45.00), 384.10 (% 87.00), 386.05 (% 34.86), 387.10 (% 7.16).

2-(2-Mercaptobenzothiazole)-N-[4-(1H-imidazol-1-yl)phenyl] acetamide (6f). Yield: 77%; m.p. 190.2–193.5°C. FTIR (ATR, cm^{-1}): 3182 (N–H), 1665 (C=O), 1608–1423 (C=C and C=N), 835 (1,4-disubstituted benzene). ^{1}H-NMR (500 MHz) (DMSO-d_6) δ (ppm): 4.24 (2H, s, CH_2-S), 7.35 (1H, s, imidazole, C_5-H), 7.36 (1H, t, J = 7.0 Hz, benzothiazole, C_5-H), 7.48 (1H, t, J = 7.0 Hz, benzothiazole C_6-H), 7.60 (2H, d, J = 9.0 Hz, phenyl $C_{2,6}$-H), 7.68 (1H, s, imidazole, C_4-H), 7.72 (2H, d, J = 9.0 Hz, phenyl, $C_{3,5}$-H), 7.83 (1H, d, J = 8.0 Hz, benzothiazole C_7-H), 8.03 (1H, d, J = 8.0 Hz, benzothiazole C_6-H), 8.19 (1H, s, imidazole C_2-H), 10.61 (1H, s, NH-CO). ^{13}C-NMR (125 MHz, DMSO-d_6) δ (ppm): 37.7, 118.0, 120.2, 120.9, 121.1, 121.9, 124.5, 126.4, 129.7, 132.5, 134.8, 135.4, 137.5, 152.5, 165.3, 166.0. LCMS (ESI) *m/z*: 184.55 (% 100.00), 367.10 (% 89.12), 368.05 (% 35.96), 369.10 (% 6.10).

2-(2-Mercapto-5-methoxybenzothiazol)-N-[4-(1H-imidazol-1-yl)phenyl]acetamide (6g). Yield: 65%; m.p. 146.7–150.2°C. FTIR (ATR, cm^{-1}): 3244 (N–H), 1649 (C=O), 1604–1452 (C=C and C=N), 833 (1,4-disubstituted benzene). ^{1}H-NMR (500 MHz) (DMSO-d_6) δ (ppm): 3.82 (3H, s, OCH_3), 4.40 (2H, s, CH_2-S), 7.00 (1H, dd, J = 8.5 Hz, J = 2.5 Hz, benzothiazole C_6-H), 7.09 (1H, s, imidazole, C_5-H), 7.37 (1H, d, J = 2.5 Hz, benzothiazole C_3-H), 7.61 (2H, d, J = 9.0 Hz, phenyl, $C_{3,5}$-H), 7.68 (1H, s, imidazole, C_4-H), 7.72 (2H, d, J = 9.0 Hz, phenyl, $C_{2,6}$-H), 7.89 (1H, s, J = 8.5 Hz, benzothiazole C_7-H), 8.19 (1H, s, imidazole C_2-H), 10.59 (1H, s, NH-CO). ^{13}C-NMR (125 MHz, DMSO-d_6) δ (ppm): 37.6, 55.5, 104.6, 113.7, 118.0, 120.2, 120.9, 122.1, 126.3, 129.7, 132.5, 135.4, 137.5, 153.8, 158.7, 165.3 167.0. LCMS (ESI) *m/z*: 199.55 (% 100.00), 397.10 (% 92.17), 398.05 (% 33.06), 399.10 (% 6.80).

2-(2-Mercapto-5-chlorobenzothiazole)-N-[4-(1H-imidazol-1-yl)phenyl]acetamide (6h). Yield: 58%; m.p. 207.8–210.3°C. FTIR (ATR, cm^{-1}): 2987 (N–H), 1680 (C=O), 1612–1425 (C=C and C=N), 839 (1,4-disubstituted benzene). ^{1}H-NMR (500 MHz) (DMSO-d_6) δ (ppm): 4.43 (2H, s, CH_2-S), 7.09 (1H, t, J = 1.0 Hz, imidazole C_5-H), 7.42 (1H, dd, J = 8.5 Hz, J = 2.0 Hz, benzothiazole, C_6-H), 7.60 (2H, d, J = 9.0 Hz, phenyl $C_{2,6}$-H), 7.68 (1H, t, J = 1.0 Hz, imidazole C_4-H), 7.73 (2H, d, J = 9.0 Hz, phenyl $C_{3,5}$-H), 7.89 (1H, d, J = 2.0 Hz, benzothiazole C_4-H), 8.06 (1H, d, J = 8.5 Hz, benzothiazole C_7-H), 8.19 (1H, t, J = 1.0 Hz, imidazole C_2-H), 10.62 (1H, s, NH-CO). ^{13}C-NMR (125 MHz, DMSO-d_6) δ (ppm): 37.8, 118.0, 120.2, 120.5, 120.9, 123.3, 124.5, 129.7, 131.2, 132.5, 133.6, 135.4, 137.4, 153.4, 165.2, 169.0. LCMS (ESI) *m/z*: 201.45 (% 100.00), 202.30 (% 42.07), 401.05 (% 93.16), 402.10 (% 11.80), 403.05 (% 35.16).

2-(2-Mercapto-1-methylimidazole)-N-[4-(1H-imidazol-1-yl) phenyl]acetamide (6i). Yield: 81%; m.p. 103.2–106.9°C. FTIR (ATR, cm^{-1}): 3140 (N–H), 1697 (C=O), 1620–1421 (C=C and C=N), 833 (1,4-disubstituted benzene). ^{1}H-NMR (500 MHz) (DMSO-d_6) δ (ppm): 3.61 (3H, s, CH_3), 3.89 (2H, s, CH_2-S), 6.97 (1H, d, J = 1.0 Hz, *N*-methylimidazole C_4-H), 7.10 (1H, s, imidazole, C_5-H), 7.26 (1H, d, J = 1.0 Hz, *N*-methylimidazole C_5-H), 7.58 (2H, d, J = 9.0 Hz, phenyl $C_{2,6}$-H), 7.67 (3H, d, J = 9.0 Hz, phenyl $C_{3,5}$-H, imidazole C_4-H), 8.19 (1H, s, imidazole C_2-H), 10.52 (1H, s, NH-CO). ^{13}C-NMR (125 MHz, DMSO-d_6) δ (ppm): 33.0, 38.3, 118.0, 120.0, 120.9, 123.6, 128.5, 129.6, 132.3, 135.4, 137.6, 139.5, 166.6. LCMS (ESI) *m/z*: 157.65 (% 100.00), 314.30 (% 88.16), 315.05 (% 23.16), 316.10 (% 9.78).

2-(2-Mercapto-5-methyl-1,3,4-thiadiazole)-N-[4-(1H-imidazol-1-yl)phenyl]acetamide (6j). Yield: 72%; m.p. 225.6–228.9°C. FTIR (ATR, cm^{-1}): 3207 (N–H), 1686 (C=O), 1622–1423 (C=C and C=N), 833 (1,4-disubstituted benzene). ^{1}H-NMR (500 MHz) (DMSO-d_6) δ (ppm): 2.68 (3H, s, CH_3), 4.29 (2H, s, CH_2-S), 7.09 (1H, s, imidazole, C_5-H), 7.60 (2H, d, J = 9.0 Hz, phenyl $C_{2,6}$-H), 7.68 (2H, d, J = 9.0 Hz, phenyl, $C_{3,5}$-H), 7.71 (1H, s, imidazole C_4-H), 8.19 (1H, s, imidazole C_2-H), 10.54 (1H, s, NH-CO). ^{13}C-NMR (125 MHz, DMSO-d_6) δ (ppm): 15.2, 38.1, 118.0, 120.1, 120.9, 129.7, 132.5, 135.4, 137.7, 164.3, 165.4, 165.7. LCMS (ESI) *m/z*: 167.65 (% 100.00), 332.30 (% 89.10), 333.05 (% 18.21), 334.10 (% 5.78).

2-(3-Mercapto-1,2,4-triazol)-N-[4-(1H-imidazol-1-yl)phenyl] acetamide (6k). Yield: 71%; m.p. 169.2–173.8°C. FTIR (ATR, cm^{-1}): 3275 (N–H), 1676 (C=O), 1614–1419 (C=C and C=N), 840 (1,4-disubstituted benzene). ^{1}H-NMR (500 MHz) (DMSO-d_6) δ (ppm): 4.07 (2H, s, CH_2-S), 7.09 (1H, t, J = 1.0 Hz, imidazole, C_5-H), 7.59 (2H, d, J = 9.0 Hz, phenyl $C_{2,6}$-H), 7.68 (1H, t, J = 1.0 Hz, imidazole C_4-H), 7.70 (2H, d, J = 9.0 Hz, phenyl $C_{3,5}$-H), 8.18 (1H, s, imidazole C_2-H), 8.46 (1H, s, 1,2,4-triazole, $C_{3,5}$-H), 10.45 (1H, s, NH-CO), 14.07 (1H, s, 1,2,4-triazole, N–H). ^{13}C-NMR (125 MHz, DMSO-d_6) δ (ppm): 36.3, 97.5, 118.0, 120.0, 120.9, 129.7, 132.3, 135.4, 137.7, 160.3, 166.4. LCMS (ESI) *m/z*: 151.45 (% 100.00), 301.30 (% 94.62), 302.10 (% 19.89), 303.15 (% 5.66).

2-(3-Mercapto-4-methyl-4H-1,2,4-triazole)-N-[4-(1H-imidazol-1-yl)phenyl]acetamide (6l). Yield: 81%; m.p. 230.5–234.8°C. FTIR (ATR, cm^{-1}): 2983 (N–H), 1681 (C=O), 1620–1415 (C=C and C=N), 839 (1,4-disubstituted benzene). ^{1}H-NMR (500 MHz) (DMSO-d_6) δ (ppm): 3.61 (3H, s, CH_3), 4.08 (2H, s, CH_2-S), 7.09 (1H, t, J = 1.0 Hz, imidazole, C_5-H), 7.60 (2H, d, J = 9.0 Hz, phenyl $C_{2,6}$-H), 7.66–7.68 (3H, m, phenyl, $C_{3,5}$-H, imidazole C_4-H), 8.18 (1H, imidazole C_2-H), 8.56 (1H, s, 1,2,4-triazole C_5-H), 10.47 (1H, s, NH-CO). ^{13}C-NMR (125 MHz, DMSO-d_6) δ (ppm): 30.8, 37.7, 118.0, 120.1, 120.9, 129.7, 132.4, 135.4, 137.5, 146.2, 148.6, 165.9. LCMS (ESI) *m/z*: 158.35 (% 100.00), 315.20 (% 89.22), 316.10 (% 17.12), 317.15 (% 6.32).

2-(5-Mercapto-1-methyl-1H-tetrazole)-N-[4-(1H-imidazol-1-yl)phenyl]acetamide (6m). Yield: 76%; m.p. 225.1–229.3°C. FTIR (ATR, cm^{-1}): 3265 (N–H), 1680 (C=O), 1618–1425 (C=C and C=N), 831 (1,4-disubstituted benzene). ^{1}H-NMR (500 MHz) (DMSO-d_6) δ (ppm): 3.99 (3H, s, CH_3), 4.31 (2H, s, CH_2-S), 7.09 (1H, s, imidazole, C_5-H), 7.59 (2H, d, J = 9.0 Hz, phenyl $C_{2,6}$-H), 7.67–7.69 (3H, m, phenyl, $C_{3,5}$-H, imidazole C_4-H), 8.18 (1H, s, imidazole C_2-H), 10.55 (1H, s, NH-CO). ^{13}C-NMR (125 MHz, DMSO-d_6) δ (ppm): 33.7, 37.6, 118.0, 120.2, 120.9, 129.7, 132.5, 135.4, 137.3, 153.3, 165.1. LCMS (ESI) *m/z*: 158.35 (% 100.00), 316.20 (% 92.27), 317.15 (% 15.33), 318.05 (% 6.12).

2-(2-Mercaptopyrimidin)-N-[4-(1H-imidazol-1-yl)phenyl] acetamide (6n). Yield: 73%; m.p. 147.4–150.6°C. FTIR (ATR, cm^{-1}): 3304 (N–H), 1658 (C=O), 1610–1425 (C=C and C=N), 831 (1,4-disubstituted benzene). ^{1}H-NMR (500 MHz) (DMSO-d_6) δ (ppm): 4.15 (2H, s, CH_2-S), 7.23 (1H, t, J = 5.0 Hz, pyrimidin, C_5-H), 7.34 (1H, s, imidazole, C_5-H), 7.64 (2H, d, J = 9.0 Hz, phenyl $C_{2,6}$-H), 7.76 (2H, d, J = 9.0 Hz, phenyl $C_{3,5}$-H), 7.85 (1H, s, imidazole C_4-H), 8.64–8.66 (3H, m, pyrimidin $C_{4,6}$-H, imidazole C_2-H), 10.60 (1H, s, NH-CO). ^{13}C-NMR (125 MHz, DMSO-d_6) δ (ppm): 33.0, 117.4, 118.9, 120.0, 121.4, 126.9, 131.5, 135.0, 138.5, 157.8, 166.4, 170.3. LCMS (ESI) *m/z*: 156.55 (% 100.00), 312.20 (% 86.77), 313.15 (% 16.81), 314.05 (% 6.54).

Antifungal activity assays. Microbiological study was performed according to EUCAST definitive method EDef 7.1 for *Candida* species [28]. Synthesized compounds were tested for their *in vitro* growth inhibitory activity against *C. glabrata* (ATCC 90030), *C. krusei* (ATCC 6258), *C. parapsilosis* (ATCC 22019), and *C. albicans* (ATCC 24433).

The yeasts were maintained in Roswell Park Memorial Institute medium, after an overnight incubation at 37°C. The inocula of test microorganisms adjusted to match the turbidity of a Mac Farland 0.5 standard tube as determined with a spectrophotometer, and the final inoculum size was 0.5–2.5 × 10^5 cfu/mL for antifungal assay. The test was carried out for medium at pH = 7, and twofold serial dilutions were applied. The last well on the microplates, which was containing only the inoculated broth, was kept as control, and the last well with no growth of microorganism was recorded to represent the MIC_{50} in μg/mL. For the antifungal assays, the test compounds and reference drugs were firstly dissolved in DMSO, and further dilutions were performed to the desired concentrations of 800, 400, 200, 100, 50, 25, 12.5, 6.25, 3.125, 1.56, and 0.78 μg/mL using Roswell Park Memorial Institute medium. The completed plates were incubated for 24 h, and at the end of the incubation, resazurin (20 μg/mL) was added into each well to control the growth in the wells. Final plates including microorganism strains were incubated for 2 h. MIC_{50} values were determined using microplate reader at 590-nm excitation and 560-nm emission wavelengths; MIC_{50} readings were performed twice for entire compounds. Ketoconazole and fluconazole were used as reference drugs.

Quantification of ergosterol level. Total intracellular sterols were extracted as recorded by Breivik and Owades [32] with slight modifications. In order to inoculate 50 mL of Sabouraud dextrose broth (Difco) containing 0, 0.78, 1.56, and 3.125 μg/mL of compound **5e**, fluconazole and ketoconazole utilized a single *C. krusei* colony from an overnight Sabouraud dextrose agar plate culture. The cultures were incubated for 16 h with shaking at 35°C. The stationary-phase cells were harvested by centrifugation at 2700 rpm (Hettich, Rotina 380 R, Germany) for 5 min and washed once with sterile distilled water. Three milliliters of 25% alcoholic potassium hydroxide solution was added to each pellet and vortex mixed for 1 min. Cell suspensions were transferred to sterile borosilicate glass screw-cap tubes and were incubated in an 85°C water bath for 1 h. Following incubation, tubes were allowed to cool to room temperature. Sterols were then extracted by addition of a mixture of 1 mL of sterile distilled water and 3 mL of chloroform followed by vigorous vortex mixing for 3 min. The chloroform layer was transferred to a clean borosilicate glass screw-cap tube, and 1 μL of sterol extract was injected to LCMSMS system (Shimadzu LCMS 8040, Kyoto, Japan). The mass spectrometric analysis was achieved by employing the Nexera XR UFLC system coupled to an LCMS-8040 tandem quadrupole mass spectrometer (Shimadzu, Kyoto, Japan). Labsolutions LCMS software (Shimadzu) was used to control the instruments and process the data. The Nexera UFLC system used in the analysis consisted of two pumps (LC-20ADxr), an autosampler (SIL-20ADxr), a column heater (CTO-10ASvp), and a degasser (DGU-20A5R). This instrument was equipped with ESI sources. Chromatographic separation was performed using a Shimadzu Shimpack FC-ODS C18 column (150 mm × 2.0 mm, 3 μm) at a flow rate of 0.25 mL/min in ESI source. The isocratic mobile phase consisted of acetonitrile-water 0.1% formic acid (50:50, v/v). The mass spectrometer operating parameters were optimized as follows: nebulizer gas flow, 3 L/min; drying gas flow, 15 L/min; desolvation line temperature, 250°C; and heat block temperature, 400°C in ESI source. Other parameters were tuned automatically. MRM method was optimized by using ergosterol standard stock solution with concentration of 20 μg/mL. Ergosterol quantity in negative control samples was regarded as 100%. All concentrations were analyzed in quadruplicate, and the results were expressed as mean ± standard deviation.

Prediction of ADME parameters. Physicochemical parameters of synthesized compounds (**5a–g**, **6a–n**) were calculated by using *QikProp 4.8* [35].

Molecular docking. A structure-based *in silico* procedure was applied to discover the binding modes of most active compound **5e** to 14-α-sterol demethylase enzyme active sites. The crystal structures of enzyme (PDB ID: 1EA1) [45], which was crystallized with the reference drug (fluconazole) of antibacterial activity assay, were retrieved from the Protein Data Bank server (www.pdb.org).

The structure of ligand was built using the *Schrödinger Maestro* [46] interface and then was submitted to the *Protein Preparation Wizard* protocol of the *Schrödinger Suite 2016 Update 2* [47]. The ligand was prepared by the *LigPrep 3.8* [48] to assign the protonation states at pH 7.4 ± 1.0 and the atom types, correctly. Bond orders were assigned, and hydrogen atoms were added to the structures. The grid generation was formed using *Glide 7.1* [49] program, and docking runs were performed with single precision docking mode (SP).

REFERENCES AND NOTES

[1] Ramirez-Villalva, A.; Gonzalez-Calderon, D.; Gonzalez-Romero, C.; Morales Rodriguez, M.; Jauregui-Rodriguez, B.; Cuevas-Yanez, E.; Fuentes-Benites, A. Eur J Med Chem 2015, 97, 275.

[2] Nikalje, A. P. G.; Ghodke, M. S.; Khan, F. A. K.; Sangshetti, J. N. Chin Chem Lett 2015, 26, 108.

[3] Cao, X.; Sun, Z.; Cao, Y.; Wang, R.; Cai, T.; Chu, W.; Yang, Y. J. Med Chem 2014, 57, 3687.

[4] Odds, F. C.; Brown, A. J.; Gow, N. A. Trends Microbiol 2003, 11, 272.

[5] Heeres, J.; Meerpoel, L.; Lewi, P. Molecules 2010, 15, 4129.

[6] Shaikh, M. H.; Subhedar, D. D.; Khan, F. A.; Sangshetti, J. N.; Nawale, L.; Arkile, M.; Shingate, B. B. J Heterocyclic Chem 2016, 54, 413.

[7] Zhao, D.; Zhao, S.; Zhao, L.; Zhang, X.; Wei, P.; Liu, C.; Cheng, M. Bioorg Med Chem 2017, 25, 750.

[8] Maertens, J. A. Clin Microbiol Infect 2004, 10, 1.

[9] White, T. C.; Marr, K. A.; Bowden, R. A. Clin Microbiol Rev 1998, 11, 382.

[10] Shah, J. J.; Khedkar, V.; Coutinho, E. C.; Mohanraj, K. Bioorg Med Chem Lett 2015, 25, 3730.

[11] Wani, M. Y.; Ahmad, A.; Shiekh, R. A.; Al-Ghamdi, K. J.; Sobral, A. J. Bioorg Med Chem 2015, 23, 4172.

[12] Iman, M.; Peroomian, T.; Davood, A.; Amini, M.; Sardari, A.; Azerang, P. Pharm Chem J 2016, 49(10), 687.

[13] Levya, J. W.; Hartmanb, J. H.; Perry, M. D.; Miller, G. P. J Mol Graph Model 2015, 56, 43.

[14] Sgherri, C.; Porta, A.; Castellano, S.; Pinzino, C.; Quartacci, M. F.; Calucci, L. Biochim Biophys Acta (BBA)-Biomembr 2014, 1838, 465.

[15] Ahmad, A.; Khan, A.; Manzoor, N.; Khan, L. A. Microb Pathogen 2010, 48, 35.

[16] Malik, M. A.; Al-Thabaiti, S. A.; Malik, M. A. Int J Mol Sci 2012, 13, 10880.

[17] Chauhan, K.; Sharma, M.; Singh, P.; Kumar, V.; Shukla, P. K.; Siddiqi, M. I.; Chauhan, P. M. Chem Comm 2012, 3, 1104.

[18] Liang, Z.; Xu, H.; Tian, Y.; Guo, M.; Su, X.; Guo, C. Molecules 2016, 21, 732.

[19] Ozkirimli, S.; Apak, T. I.; Kiraz, M.; Yegenoglu, Y. Arch Pharm Res 2005, 28, 1213.

[20] Krátký, M.; Volková, M.; Novotná, F.; Trejtnar, F.; Stolaříková, J.; Vinšová, J. Bioorg Med Chem 2014, 22, 4073.

[21] Turan-Zitouni, G.; Ozdemir, A.; Guven, K. Arch Pharm 2005, 338, 96.

[22] Turan-Zitouni, G.; Ozdemir, A.; Kaplancikli, Z. A. Phosphorus Sulfur Silicon Relat Elem 2005, 180, 2717.

[23] Kumar, S. T. V. S. K.; Kumar, L.; Sharma, V. L.; Jain, A.; Jain, R. K.; Maikhuri, J. P.; Kumar, M.; Shukla, P. K.; Gupta, G. Eur J Med Chem 2008, 43, 2247.

[24] Kumar, L.; Sarswat, A.; Lal, N.; Sharma, V. L.; Jain, A.; Kumar, R.; Gupta, G. Eur J Med Chem 2010, 45, 817.

[25] Karaburun, A. Ç.; Kaplancikli, Z. A.; Gundogdu-Karaburun, N.; Demirci, F. Lett Drug Des Discov 2011, 8, 811.

[26] Ge, Z.; Ji, Q.; Chen, C.; Liao, Q.; Wu, H.; Liu, X.; Liao, F. J. Med Chem 2016, 31, 219.

[27] Yurttaş, L.; Özkay, Y.; Duran, M.; Turan-Zitouni, G.; Özdemir, A.; Cantürk, Z.; Kaplancıklı, Z. A. Phosphorus Sulfur Silicon Relat Elem 2016, 191, 1166.

[28] EUCAST. Definitive document EDef 7.1: method for the determination of broth dilution MICs of antifungal agents for fermentative yeasts 2008.

[29] Borra, R. C.; Lotufo, M. A.; Gagioti, S. M.; Barros, F. D. M.; Andrade, P. M. Braz Oral Res 2009, 23, 255.

[30] Palomino, J. C.; Martin, A.; Camacho, M.; Guerra, H.; Swings, J.; Portaels, F. Antimicrob Agents Chemother 2002, 46, 2720.

[31] Dhingra, S.; Cramer, R. A. Front Microbiol 2017, 8.

[32] Zhang, Y. Q.; Rao, R. Virulence 2010, 1, 551.

[33] Breivik, O. N.; Owades, J. L. Agric Food Chem 1957, 5, 360.

[34] De Waterbeemd, H. V.; Gifford, E. Nat Rev Drug Discov 2013, 2, 192.

[35] QikProp, Version 4.8; Schrödinger, LLC: New York, NY, 2016.

[36] Lipinski Christopher, A.; Franco, L.; Dominy Beryl, W.; Feeney Paul, J. Adv Drug Deliv Rev 2001, 46, 3.

[37] Jorgensen, W. L.; Duffy, E. M. Adv Drug Deliv Rev 2002, 54, 355.

[38] Larissa, M. P.; Thomas, L. P.; Michael, R. PNAS 2001, 98, 3068.

[39] Saeed, E.; Touba, B.; Hamid, I.; Alireza, F.; Mehraban, F.; Mahtab, A. K.; Somaye, S. J. Enzyme Inhib Med Chem 2014, 29, 263.

[40] Rodolfo, G. C.; Roberto, M.; María Eugenia, T. B.; Marco, G.; Marco Martín, G. C. Chem Pharm Bull 2014, 62, 16.

[41] Reena, G.; Subhash, A.; Sudhir, A. K. Bioorg Med Chem 2004, 12, 2937.

[42] Armando, R.; Simone, B.; Annalina, L.; Marco, M.; Adriano, M.; Simona, R.; Esperanza, H.; Bruno, M. J Med Chem 2002, 45, 4903.

[43] Kantam, M. L.; Ramani, T.; Chakrapani, L. Synth Commun 2008, 38, 626.

[44] Venuti, M. C.; Stephenson, R. A.; Alvarez, R.; Bruno, J. J.; Strosberg, A. M. J Med Chem 1988, 31, 2136.

[45] Karaca Gençer, H.; Acar Çevik, U.; Levent, S.; Sağlık, B. N.; Korkut, B.; Özkay, Y.; Ilgın, S.; Öztürk, Y. Molecules 2017, 22, 507.

[46] Maestro, Version 10.6; Schrödinger, LLC: New York, NY, 2016.

[47] Schrödinger, LLC, Version 2016-2; New York, NY, 2016.

[48] LigPrep, Version 3.8; Schrödinger, LLC: New York, NY, 2016.

[49] Glide, Version 7.1; Schrödinger, LLC: New York, NY, 2016.

SUPPORTING INFORMATION

Additional supporting information may be found online in the Supporting Information section at the end of the article.